

Departure from BCS response in photoexcited superconducting NbN films observed by terahertz spectroscopy

M. Šindler,¹ C. Kadlec,² P. Kužel,² K. Ilin,³ M. Siegel,³ and H. Němec^{2,*}

¹*Institute of Physics, Czech Academy of Sciences, Cukrovarnická 10, 16253 Prague 6, Czech Republic*

²*Institute of Physics, Czech Academy of Sciences, Na Slovance 2, 18221 Prague 8, Czech Republic*

³*Institut für Mikro- und Nanoelektronische Systeme (IMS), Karlsruher Institut für Technologie, Hertzstraße 16, 76187 Karlsruhe, Germany*



(Received 26 July 2017; revised manuscript received 25 January 2018; published 12 February 2018)

We investigate time-resolved terahertz conductivity of thin superconducting NbN films with various thicknesses upon their excitation by intense femtosecond laser pulses. The recovery dynamics following a complete destruction of the superconducting state occurs via a growth of superconducting islands in the normal-state environment. This is in contrast with previous observations of the recovery upon strong-field terahertz excitation [R. Matsunaga and R. Shimano, *Phys. Rev. Lett.* **109**, 187002 (2012)]. We observe that the density of electronic states in the superconducting islands deviates from the BCS theory predictions on a subnanosecond time scale, while equilibrium terahertz conductivity spectra confirm the standard BCS behavior in the ground state.

DOI: [10.1103/PhysRevB.97.054507](https://doi.org/10.1103/PhysRevB.97.054507)

Nonequilibrium superconductivity has been a subject of intensive research for a long time [1,2]. Transient dynamics involving the breaking and recovery of the superconducting state can be triggered by ultrashort impulsive excitation in the optical or terahertz spectral range [3–5]. Optical excitation of a superconductor generates hot quasiparticles with a huge excess energy compared to the optical gap; these emit high-frequency phonons during their cooling, which leads to the phonon bottleneck effect [6] and to the slowing down of Cooper pair recovery. Nonthermal energetic distribution of quasiparticles developing upon optical excitation may lead to significant transient changes in the width of the optical superconducting gap [1,5]. Concurrently, intense THz excitation is able to create a high concentration of quasiparticles without heating the lattice through phonon emission [4]. Recently, it has been also shown that a transient coherent charge transport and an opening of the optical superconducting gap can be induced at temperatures far above the superconducting transition by an intense light pulse in various materials [7,8]. Understanding nonequilibrium superconductivity thus becomes essential for the achievement of transient control of various aspects of the superconducting state.

Terahertz (THz) spectroscopy enables an in-depth understanding of superconducting properties, namely, when the superconducting gap falls into the THz spectral range [9,10]. The spectral response of Cooper pairs reflects the density of states close to the superconducting gap and it fundamentally differs from that of separate quasiparticles; its temperature dependence provides a clear link to the microscopic origin of the superconductivity. Time-resolved measurements in the THz range then allow monitoring the dynamics of both Cooper pairs and quasiparticles [9,11].

In this paper, we focus on the investigation of charge dynamics and Cooper pair recovery in thin NbN layers with

thicknesses 5–30 nm. The NbN films were deposited on 1-mm-thick (100) MgO substrates by reactive magnetron sputtering of a pure Nb target in an atmosphere of argon and nitrogen gas mixture at partial pressures $P_{\text{Ar}} = 1.5 \times 10^{-3}$ mbar and $P_{\text{N}_2} = 3.3 \times 10^{-4}$ mbar. The temperature of the heater plate with substrates was 850 °C and the deposition rate of NbN was ~ 0.12 nm/s. More details about the deposition technology are in Ref. [12]. The critical temperature slightly increases with the film thickness (Table I), in agreement with previous reports [13].

Equilibrium transmission measurements of the films were performed in a standard time-domain THz spectroscopy setup based on a femtosecond laser oscillator [14]. The substrate thicknesses were carefully determined prior to the deposition of NbN films, which allowed us to minimize systematic errors [15]; the complex conductivity spectra $\tilde{\sigma}(\omega) = \sigma_1(\omega) + i\sigma_2(\omega)$ of the films (Fig. 1) were determined by numerically solving the exact formula for thin-film transmittance [16]. In the normal state ($T > T_c$) the conductivity spectrum is Drude-like $\sigma_n(\omega) = \sigma_0^{\text{eq}}/(1 - i\omega\tau)$, controlled by two parameters: a dc conductivity σ_0^{eq} and a momentum scattering time τ . In the superconducting state ($T < T_c$) all the spectra σ_s^{eq} were fitted by the model of optical conductivity of BCS superconductors derived by Zimmermann *et al.* [17], where we additionally assumed (and integrated over) a Gaussian spatial distribution of the gap values. The fitting allowed us to determine the relative optical gap at zero temperature $2\Delta(0)/(k_B T_c)$; the values are similar to those reported for other NbN films [11,18–20]. All steady-state parameters of the films are summarized in Table I. The observed spatial distribution of gap sizes [with a standard deviation of $(0.2 - 0.3) \times 2\Delta(T)/(k_B T_c)$] is broader than in the case of NbN films deposited on high-resistivity silicon [16]. It is important to notice that there are no systematic deviations of the model from the measured spectra, even for the thinnest films. Possible size effects thus affect at most the parameters of the conduction, but they preserve its BCS character. The slightly worse agreement of the real parts for

*nemec@fzu.cz

TABLE I. Parameters of the investigated samples. The film thickness d_f was measured using a stylus profiler, the critical temperature T_c was determined from the dc conductivity measurements, and the optical absorption coefficient α_{opt} was obtained from transmittance and reflectance measurements at 800 nm; σ_0^{eq} , τ , and $2\Delta(0)/k_B T_c$ were determined from fits of the THz conductivity spectra.

Sample	d_f (nm)	T_c (K)	σ_0^{eq} ($\mu\Omega^{-1}\text{m}^{-1}$)	τ (fs)	$2\Delta(0)/k_B T_c$	α_{opt}^{-1} (nm)
NbN-5	5.3	13.9	1.53	15	4.2	10
NbN-15	14.5	15.2	1.63	14	4.1	13
NbN-30	30.1	15.5	2.46	18	3.8	15

the NbN-5 sample is insignificant, since the accuracy of the *equilibrium* conductivity becomes worse with the decreasing film thickness [15].

Optical pump–THz probe measurements were carried out in a setup similar to the one described in Ref. [21] based on a Ti:sapphire femtosecond laser amplifier (Spitfire Ace, 5 kHz repetition rate). The THz pulses used in this work do not induce nonlinear effects since they are much weaker (peak field <5 kV/cm) than those used in Ref. [4]. The photocarrier density generated by 800-nm excitation pulses has enough time to homogenize over the entire thickness of NbN films on a picosecond time scale; for this reason we used the formula for homogeneous thin-film transmittance [15,16] to retrieve the conductivity of the photoexcited film. The linear penetration depth α_{opt}^{-1} of the excitation beam was determined from the measurement of the transmittance and reflectance of the pump beam.

We first measured the THz kinetics (Fig. 2), i.e., transient transmitted field δE in the maximum of the differential wave form $\delta E(t) = E'(t) - E_0(t)$ (where E' and E_0 are the fields transmitted through a photoexcited and nonphotoexcited sample, respectively) as a function of the pump-probe delay. During the excitation process the Cooper pairs are broken and the excess energy of the photoexcited quasiparticles is rapidly redistributed within electron and phonon subsystems;

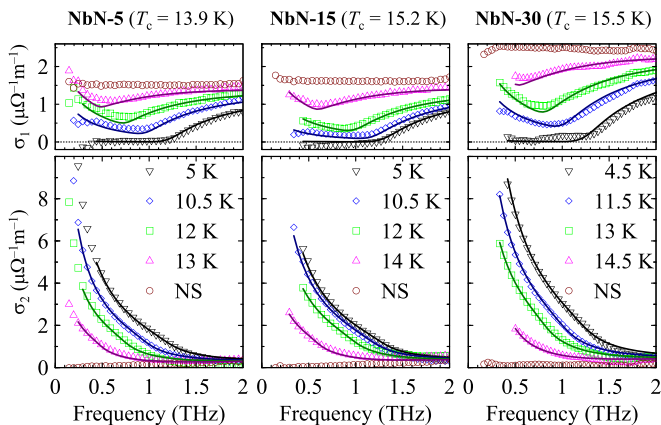


FIG. 1. Equilibrium conductivity of NbN films at several temperatures. Symbols: measured data; lines: fit by the model of optical conductivity of BCS superconductors [17] with a distribution of gap sizes. NS = normal state.

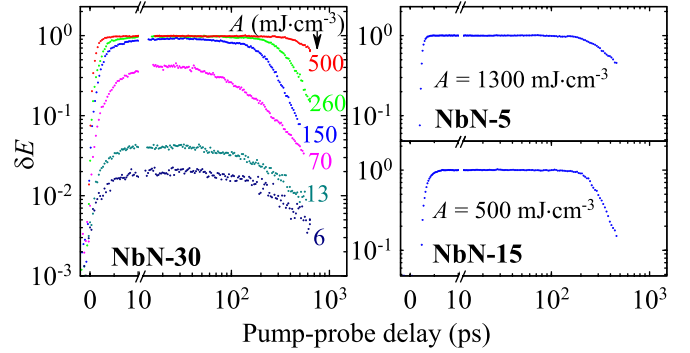


FIG. 2. Normalized differential THz field δE measured at 5 K for NbN-30, 15, and 5 for various absorbed pump energy densities A .

the accompanying local heating leads to further breaking of Cooper pairs [6] and, in turn, to a decrease of σ_2 . This process leads to a phase shift of the transmitted THz pulse observed as a rise in δE occurring within the initial ~ 20 ps [3].

Subsequently, δE exhibits a decay which reflects the recovery of the superconducting state similarly as described in Ref. [3]. For excitation densities $\gtrsim 100 \text{ mJ cm}^{-3}$ a plateau appears in the signal prior to the decay: The absorbed energy here is high enough to break all Cooper pairs and provide quasiparticles with excess energy, so that Cooper pair recovery is delayed. In this paper, we are interested in the recovery from this strong-excitation (plateau) regime. We normalize δE so that the full suppression of the superconducting state corresponds to $\delta E = 1$; also, for samples NbN-5 and NbN-15 we show only kinetics exhibiting the plateau regime in Fig. 2. Note that we did not observe any significant long-term heating of the films (even for the highest fluences used): We checked that the conductivities measured with a negative pump-probe delay were always equal to the equilibrium ones.

We now turn our attention to the THz conductivity spectra measured during the recovery dynamics (Fig. 3). These experiments were carried out at excitation powers of 5–6 mW, for which the superconducting state is fully broken without additional long-term lattice heating. Due to different thicknesses and optical absorption of the three samples, the absorbed energy density was 1.3, 0.5, and 0.15 J cm^{-3} for NbN-5, 15, and 30, respectively.

For short pump-probe delays, there is a range of frequencies (~ 0.3 – 0.5 THz) for which the real conductivity exceeds both the normal-state conductivity σ_n and the conductivity of the superconducting state in equilibrium σ_s^{eq} (discussed later in Fig. 4). Such a behavior cannot be explained within a framework of the local (microscopic) conductivity, but it can be understood as a consequence of depolarization field effects in a spatially heterogeneous system consisting of normal- and superconducting-state regions that develop during the recovery dynamics. Indeed, the real and imaginary conductivities of the two components couple in the effective properties of the mixture; this becomes especially important when the more conducting component is not percolated [22,23]. Namely, high values of the imaginary part of the conductivity in the superconducting phase can significantly enhance the real part of the effective conductivity and explain the experimental data. This suggests that the recovery process occurs through a buildup of

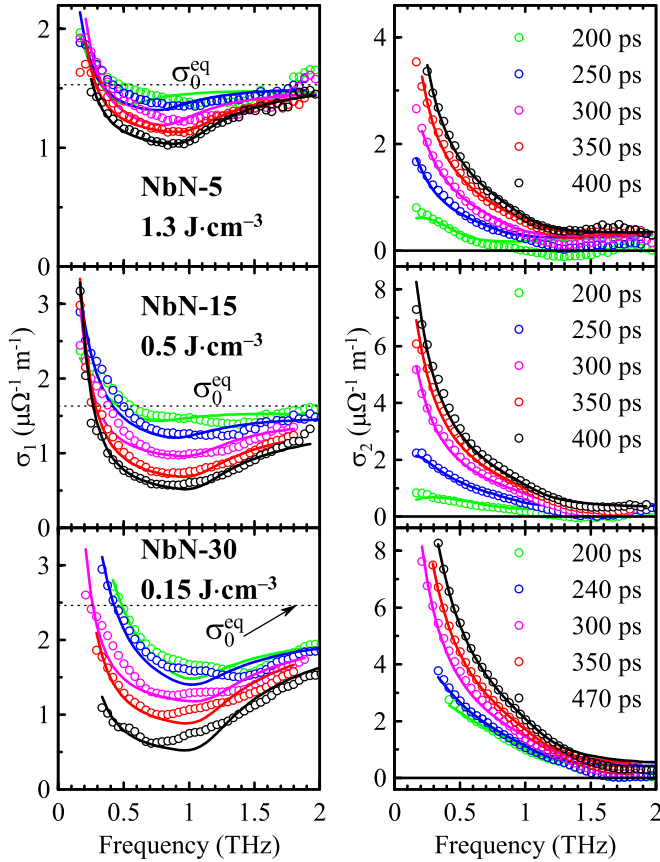


FIG. 3. Real (σ_1) and imaginary (σ_2) part of the conductivity of NbN films after photoexcitation, measured for several pump-probe delays at 5 K. The optical energy absorbed in the films is indicated. Symbols: measured data; lines: best fit by effective conductivity σ_{eff} from Eq. (1).

isolated superconducting islands in an environment filled with the normal state with the conductivity σ_n . It is important to stress that the observed spectra cannot be described by effective medium theories similar to, e.g., the Bruggeman model where the superconducting state is considered as percolated within the sample (see BG and MG-inv curves in Fig. 4). This behavior is in a sharp contrast with that observed under excitation of the superconducting state of NbN using intense THz pulses: In that case isolated normal-state regions were generated in a superconducting environment [4].

Since we know that the superconducting phase must grow from sparse nonpercolated islands we can describe the nonequilibrium effective conductivity σ_{eff} of the photoexcited NbN film by the Maxwell-Garnett (MG) model,

$$\frac{\sigma_{\text{eff}} - \sigma_n}{L\sigma_{\text{eff}} + (1-L)\sigma_n} = f_s \frac{\sigma_s - \sigma_n}{L\sigma_s + (1-L)\sigma_n}, \quad (1)$$

where f_s is the volume filling fraction of the superconducting component (with the conductivity σ_s) and L is the depolarization factor of superconducting inclusions. We assume that the conductivity of superconducting islands is described by Zimmermann's model [17] with the distribution of optical gaps identical to the one found in equilibrium.

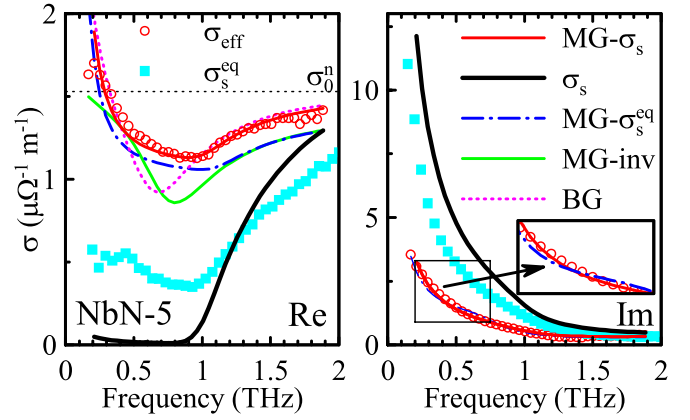


FIG. 4. Comparison of various conductivity data (symbols) and models (lines) for sample NbN-5. Experiment: σ_s^{eq} , equilibrium conductivity for $T = 10.4$ K, i.e., $\Delta = 3.32k_B T_c$. σ_{eff} , transient conductivity (at 350 ps) corresponding to a similar optical gap value, $\Delta = 3.42k_B T_c$; other conditions as in Fig. 3. Models (best fit values): MG- σ_s , final model (1) with non-BCS amplitude σ_0 ; σ_s , superconducting component retrieved from MG- σ_s ; MG- σ_s^{eq} , model (1) with BCS amplitude σ_0^{eq} ; MG-inv, MG model assuming isolated normal-phase islands in a superconducting matrix; BG, Bruggeman model. Inset: Zoom on MG- σ_s and MG- σ_s^{eq} fits of the imaginary part of the transient conductivity. For some models we plot only the real part for clarity.

Within the standard BCS theory of the superconducting state the fitting parameters—which potentially depend on the pump-probe delay—are the gap width Δ , the filling factor f_s , and the depolarization factor L . However, the fits of our experimental results do not provide a satisfactory agreement. Systematic differences between the experimental and theoretical spectra are observed, namely, for the thinnest sample (NbN-5) and for short pump-probe delays (<400 ps); in particular, we observe a mismatch between the real and imaginary part of the effective conductivity (see the fit MG- σ_s^{eq} shown in Fig. 4 as an example). We stress that this mismatch cannot be a consequence of an experimental error: The real and imaginary parts in the time-domain THz spectroscopy are determined from a single wave form; therefore, a possible error in its amplitude would scale both parts by a similar factor. The retrieval of the complex conductivity in the pump-probe experiment uses the unexcited sample as a reference, therefore, the uncertainty in the substrate thickness does not compromise in any way the retrieved conductivity. In this sense, the ratio between the real and imaginary part here is determined more accurately than in the case of the equilibrium conductivities, which critically rely on a determination of the substrate thickness [15].

For this reason we included into the fitting procedure an additional free parameter σ_0 , which characterizes the amplitude of the BCS conductivity following Ref. [17] (curve MG- σ_s in Fig. 4). In our view, the sample is composed of two kinds of spatially separated nanoscopic regions: (1) regions in the normal state, characterized by the Drude conductivity σ_n with amplitude σ_0^{eq} given by equilibrium conditions, and (2) regions in the superconducting state σ_s , where both superconducting pairs and quasiparticles can exist. According to the standard

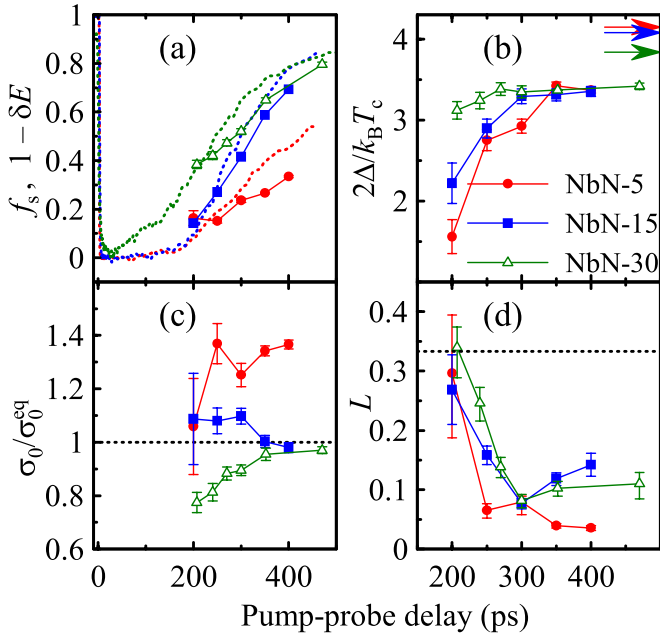


FIG. 5. Symbols: Fitted properties of the transient superconducting state as a function of the pump-probe delay. Excitation conditions are the same as in Fig. 3; $T = 5$ K. (a) Symbols represent f_s , whereas the dotted lines indicate the normalized signal $1 - \delta E$, which can be viewed as a rough estimate of the superconducting fraction. (b)–(d) Symbols: fitted parameters; the lines only serve to guide the eye. The arrows in (b) indicate the equilibrium gap widths at 5 K. The dotted line in (d) corresponds to the depolarization factor of spherical inclusions.

BCS model we should have $\sigma_0 \equiv \sigma_0^{\text{eq}}$ in these islands, which leads to a mismatch with the experiment as mentioned above. This mismatch is avoided when we consider σ_0 different from the equilibrium value σ_0^{eq} : This difference then represents the departure of our system from the BCS behavior, as discussed below. This approach significantly improves the fits which now correctly reproduce the main features of the measured spectra (compare the MG- σ_s^{eq} and MG- σ_s curves in Fig. 4).

The behavior of the fitting parameters is summarized in Fig. 5. We plot here only results obtained at long pump-probe delays ($\gtrsim 200$ ps), for which the contribution of the superconducting component is significant: This is a prerequisite for a reliable determination of all fitting parameters.

In agreement with the expectations, the recovery dynamics is represented by an increasing fraction of the superconducting component f_s [Fig. 5(a)]; this means that new superconducting islands are formed and/or their size grows in time. In the early phase (~ 200 ps), the depolarization factor $L \approx 1/3$ [Fig. 5(d)], which corresponds to isolated spherical islands. This can be understood by the fact that the size of the islands is smaller than or comparable to the thickness of the NbN film. Subsequently, the depolarization factor decreases and tends to values around 0.1 at high pump-probe delays; this effect is the most markedly observed in the case of the thinnest film [Fig. 5(d)]. This indicates that the recovery dynamics is connected to a growth of the superconducting islands in size into more complex in-plane structures which tend to form a network close to the percolation [24]. This scenario is thus different from that observed under

excitation by intense THz pulses [4], where the percolation of the superconducting phase was reported.

Note that the Bruggeman effective medium approach employed in Ref. [4] is an approximation in which the percolation threshold is strictly connected to the filling factor; it is then hard to distinguish whether the observed behavior is due to the percolation, or due to the filling factor growth. In contrast, the MG approach employed in this work permits controlling the filling factor arbitrarily while maintaining the nonpercolated state.

The increase of the optical gap width [Fig. 5(b)] is initially (at ~ 200 ps) faster than the recovery of the superconducting population [Fig. 5(a)]. However, although the gap size approaches a quasisteady value at about 400 ps, this value remains significantly different from the equilibrium one. It implies that, in the final stage, the superconducting population recovers faster (on a sub-ns time scale) while the properties of the superconducting state (represented here by the optical gap) return back to equilibrium at least within nanoseconds. The initial change in the gap size is more pronounced for samples NbN-5 and NbN-15, where the absorbed energy density is higher, while it is weaker in sample NbN-30.

The number of electrons should be conserved when the system undergoes the superconducting transition; this imposes specific conditions on the conductivity spectra. In particular, within the BCS theory the Drude conductivity amplitude in the normal state is equal to the conductivity amplitude in the superconducting state, and both are denoted by σ_0 in Zimmermann's work [17]; here, for convenience, we introduced the symbol σ_0^{eq} to denote these values in equilibrium.

The same conservation law should apply also for the photoinduced transition during the recovery process, although the electrons in the inhomogeneous photoexcited sample are distributed among two states separated in space: the normal state forming the matrix (which is still locally described by the Drude conductivity amplitude σ_0^{eq}), and the superconducting islands with the conductivity amplitude σ_0 . We clearly observe that $\sigma_0 \neq \sigma_0^{\text{eq}}$ [see Fig. 5(c)]. This phenomenon must be explained by a transfer of the spectral weight (i.e., of the density of electron states) between the spectral range where the conductivity measurements have been performed and another region at higher frequencies, which implies that the density of nonequilibrium electron states does not follow the conventional BCS theory. On the other hand, a low-frequency region (below our spectral range) cannot be involved in this transfer since, in such a case, a further adjustment of the ratio between the real and imaginary part of the superconducting component σ_s would be needed owing to the Kramers-Kronig relations to match the observed spectrum.

Our experimental results show that the deviation from the BCS density of states strongly depends on the film thickness. In NbN-30 at times shorter than ≈ 300 ps we find that $\sigma_0 < \sigma_0^{\text{eq}}$, i.e., the spectral weight is transferred from our range towards higher frequencies; at longer times, σ_0 approaches σ_0^{eq} . The effect is only slightly pronounced in the 15-nm film: This is in agreement with an extensive work on NbN films with a similar thickness, where no deviation from the BCS response has been observed [3]. Finally, in NbN-5, σ_0 progressively increases above σ_0^{eq} (the spectral weight is transferred from high frequencies towards the THz spectral region) and we even do

not observe any signatures of its recovery for times as long as 500 ps.

Size effects induced by the film thickness thus seem to control the photoinduced nonequilibrium density of states. In Ref. [25] it was shown that a strong disorder adds some spectral weight inside the optical gap. However, depending on the sample thickness, we observe either a positive or negative sign in the changes of the spectral weight—this seems to rule out the disorder as the effect responsible for the non-BCS conductivity spectra. This finding may provide a stimulus for the theoretical explanation of the phenomenon.

In Fig. 4 we compare a transient spectrum σ_s of the superconductive component (black line) and an equilibrium spectrum σ_s^{eq} (cyan symbols) measured at a temperature chosen such that the optical gaps corresponding to these two measurements acquire very similar values. However, the two spectra significantly differ from each other, which demonstrates the joint effect of the heterogeneity and of the spectral weight shift in the transient regime.

In summary, we investigated thin superconducting NbN films with various thicknesses by time-resolved terahertz spec-

troscopy. In agreement with previous reports, the equilibrium THz conductivity can be described by the BCS theory. Upon strong photoexcitation by femtosecond laser pulses, when the superconducting state is completely broken, the recovery dynamics occurs by a growth of initially spherical isolated superconducting islands in the normal-state environment. These islands subsequently merge towards a nearly percolated superconducting network. The recovery process is accompanied by a shift in the conductivity spectral weight, indicating a departure from the BCS character of the density of electron states in these islands. While the superconductivity recovers on the hundreds-picosecond time scale, the properties characterizing the superconducting state (such as the gap width and the density of states) recover much more slowly, at least on the nanosecond time scale.

We acknowledge the financial support by the Czech Science Foundation (Project No. 17-04412S). Technical support by V. Skoromets and V. Zajac during THz experiments and fruitful discussions with J. Koláček and P. Lipavský are also acknowledged.

-
- [1] T. Kommers and J. Clarke, *Phys. Rev. Lett.* **38**, 1091 (1977).
 [2] A. Rothwarf and B. N. Taylor, *Phys. Rev. Lett.* **19**, 27 (1967).
 [3] M. Beck, M. Klammer, S. Lang, P. Leiderer, V. V. Kabanov, G. N. Goltsman, and J. Demsar, *Phys. Rev. Lett.* **107**, 177007 (2011).
 [4] R. Matsunaga and R. Shimano, *Phys. Rev. Lett.* **109**, 187002 (2012).
 [5] M. Beck, I. Rousseau, M. Klammer, P. Leiderer, M. Mittendorff, S. Winnerl, M. Helm, G. N. Goltsman, and J. Demsar, *Phys. Rev. Lett.* **110**, 267003 (2013).
 [6] V. V. Kabanov, J. Demsar, and D. Mihailovic, *Phys. Rev. Lett.* **95**, 147002 (2005).
 [7] M. Mitrano, A. Cantaluppi, D. Nicoletti, S. Kaiser, A. Perucchi, S. Lupi, P. Di Pietro, D. Pontiroli, M. Riccò, S. R. Clark, D. Jaksch, and A. Cavalleri, *Nature (London)* **530**, 461 (2016).
 [8] W. Hu, S. Kaiser, D. Nicoletti, C. R. Hunt, I. Gierz, M. C. Hoffmann, M. Le Tacon, T. Loew, B. Keimer, and A. Cavalleri, *Nat. Mater.* **13**, 705 (2014).
 [9] R. D. Averitt and A. J. Taylor, *J. Phys.: Condens. Matter* **14**, R1357 (2002).
 [10] R. A. Kaindl, M. A. Carnahan, J. Orenstein, D. S. Chemla, H. M. Christen, H.-Y. Zhai, M. Paranthaman, and D. H. Lowndes, *Phys. Rev. Lett.* **88**, 027003 (2001).
 [11] U. S. Pracht, E. Heintze, C. Clauss, D. Hafner, R. Bek, D. Werner, S. Gelhorn, M. Scheffler, M. Dressel, D. Sherman, B. Gorshunov, K. S. Il'in, D. Henrich, and M. Siegel, *IEEE Trans. THz Sci. Technol.* **3**, 269 (2013).
 [12] D. Henrich, S. Dörner, M. Hofherr, K. Il'in, A. Semenov, E. Heintze, M. Scheffler, M. Dressel, and M. Siegel, *J. Appl. Phys.* **112**, 074511 (2012).
 [13] A. Semenov, B. Günther, U. Böttger, H.-W. Hübers, H. Bartolf, A. Engel, A. Schilling, K. Ilin, M. Siegel, R. Schneider, D. Gerthsen, and N. A. Gippius, *Phys. Rev. B* **80**, 054510 (2009).
 [14] P. Kužel, H. Němec, F. Kadlec, and C. Kadlec, *Opt. Express* **18**, 15338 (2010).
 [15] C. Kadlec, F. Kadlec, H. Němec, P. Kužel, J. Schubert, and G. Panaitov, *J. Phys.: Condens. Matter* **21**, 115902 (2009).
 [16] M. Šindler, R. Tesař, J. Koláček, P. Szabó, P. Samuely, V. Hašková, C. Kadlec, F. Kadlec, and P. Kužel, *Supercond. Sci. Technol.* **27**, 055009 (2014).
 [17] W. Zimmermann, E. H. Brandt, M. Bauer, E. Seider, and L. Genzel, *Physica C* **183**, 99 (1991).
 [18] L. Kang, B. B. Jin, X. Y. Liu, X. Q. Jia, J. Chen, Z. M. Ji, W. W. Xu, P. H. Wu, S. B. Mi, A. Pimenov, Y. J. Wu, and B. G. Wang, *J. Appl. Phys.* **109**, 033908 (2011).
 [19] Y. Ikebe, R. Shimano, M. Ikeda, T. Fukumura, and M. Kawasaki, *Phys. Rev. B* **79**, 174525 (2009).
 [20] Y. Noat, V. Cherkez, C. Brun, T. Cren, C. Carbillet, F. Debontridder, K. Ilin, M. Siegel, A. Semenov, H.-W. Hübers, and D. Roditchev, *Phys. Rev. B* **88**, 014503 (2013).
 [21] L. Fekete, P. Kužel, H. Němec, F. Kadlec, A. Dejnek, J. Stuchlík, and A. Fejfar, *Phys. Rev. B* **79**, 115306 (2009).
 [22] H. Němec, P. Kužel, and V. Sundström, *J. Photochem. Photobiol. A* **215**, 123 (2010).
 [23] E. Hendry, M. Koeberg, B. O'Regan, and M. Bonn, *Nano Lett.* **6**, 755 (2006).
 [24] H. Němec, V. Zajac, I. Rychetský, D. Fattakhova-Rohlfing, B. Mandlmeier, T. Bein, Z. Mics, and P. Kužel, *IEEE Trans. THz Sci. Technol.* **3**, 302 (2013).
 [25] G. Seibold, L. Benfatto, and C. Castellani, *Phys. Rev. B* **96**, 144507 (2017).